ARTICLES

Salt-Induced Aggregation of Polystyrene Latex Particles in Aqueous Solutions of a Hydrophobically Modified Nonionic Cellulose Derivative and Its Unmodified Analogue

Anna-Lena Kjøniksen,[‡] Fredrik Joabsson,[†] Krister Thuresson,[†] and Bo Nyström*,[‡]

Department of Chemistry, University of Oslo, P.O. Box 1033, N-0315 Oslo, Norway, and Physical Chemistry 1, Chemical Center, Lund University, P.O. Box 124, S-221 00 Lund, Sweden

Received: February 24, 1999

The structure and kinetics of clusters formed in the salt-induced (0.7 M NaCl) aggregation processes of polystyrene latex particles in the presence of various amounts of ethyl(hydroxyethyl)cellulose (EHEC) or the hydrophobically modified analogue (HM-EHEC) have been investigated with the aid of light scattering measurements. Under all conditions, both with and without polymer, the aggregating clusters are well described by a fractal geometry with a fractal dimension of 2.1. Three stages can be discerned in the salt-induced aggregation process of bare latex particles. In the early stage, the time evolution of the hydrodynamic radius R_h can be described by a power law $R_h \propto t^{0.04}$, followed by a steep transition zone and an exponential growth at long times. In the presence of polymer, the slow cluster size growth can be described by the above power law over the whole considered time domain. The value of the power law exponent is independent of polymer concentration and hydrophobicity of the polymer. The results show that only a small amount of adsorbed polymer is needed to slow the rate of the aggregation process. The results show that both polymers adsorb to the latex particles, but the adsorption is more pronounced for the hydrophobically modified polymer.

Introduction

Polymer adsorption on colloidal particles and aggregation of these particles are phenomena that have attracted a great deal of interest[1−6] in recent years. The stabilization of colloidal particles by anchored polymers is an attractive approach to improve paints, coatings, inks, and magnetic media.[1] Detailed understanding of polymer adsorption and aggregation rests upon knowledge of the intermolecular forces between polymers and colloidal particles and how these interactions are affected by environmental conditions such as the thermodynamic quality of the immersion solvent and salinity.

A typical aqueous colloidal dispersion consists of particles whose stability is controlled by the presence of some surface charge. The suppression of this stabilizing effect can be achieved by the addition of moderate amounts of an inert electrolyte. Aggregation may be induced by addition of, e.g., NaCl, which decreases the Debye−Hückel screening length, thereby decreasing the repulsive barrier between the particles. A great deal of interest, both from a theoretical[7−11] and an experimental[12−22] point of view, has been devoted to study the aggregation of colloidal particles, especially the structure of colloidal aggregates and the kinetics of their formation. The general accepted picture is that there are two limiting behaviors both for the reaction kinetics and for the morphology of the aggregates. The two limiting regimes of irreversible colloid aggregation have been identified as diffusion-limited cluster−cluster aggregation[8,23] (DLCA) and reaction-limited cluster−cluster aggregation[7,24] (RLCA). These two regimes have been studied theoretically, by computer simulation and by experimental studies of various colloids. Each regime is distinguished by several distinct and characteristic features. The structures of the clusters in both regimes can be characterized by their fractal dimension d_f, i.e., the exponent that relates the total mass M of the aggregate to its typical size R, $M \sim R^d$f. Fractal morphology has already been demonstrated for a range of particle aggregates including those of silica, gold, polystyrene latex, and clay, among others. It has been argued[18] from experimental observations that these limiting regimes of colloid aggregation are universal, independent of the chemical details of the particular colloid system.

The parameter that determines which regime is to be expected is the particle sticking efficiency, that is, the potential energy barrier to aggregation. DLCA behavior occurs when the sticking probability is equal to one, whereby collision between particles always resulted in irreversible sticking, and the aggregation rate is limited solely by the time taken for clusters to encounter each other by diffusion. The DLCA model was found to produce aggregates of very open structures with $d_f \approx 1.8$ for three-dimensional systems, and the kinetics is characterized by a power law growth[25] in the form of $R \sim t^{1/d_f}$, where t is time. If the sticking probability (or collision efficiency) is very small, the clusters will need to collide many times before they stick, and as a result the diffusing clusters are allowed to penetrate further into each other before sticking. This type of aggregation gives rise to RLCA, and simulations[9] show an increase in the fractal dimension over the diffusion-limited case with $d_f \approx 2.1$ (i.e., denser aggregates). This process exhibits exponential

‡ University of Oslo.
† Lund University.
* Corresponding author.

10.1021/jp990669w CCC: $18.00
Published on Web 10/26/1999

kinetics[25] with $R \sim \exp(bt)$, where b is a constant dependent on the experimental conditions.

The RLCA behavior is frequently reported for salt-induced aggregation of suspensions of polystyrene latices at moderate levels of salt addition,[18,20] suggesting that there is still a substantial, but not insurmountable, repulsive force between the particles, so that the aggregation rate is limited by the time taken for two clusters to overcome this repulsive barrier by thermal activation. At higher salt concentrations, when there is negligible repulsive force between the colloid particles, the DLCA model is often found[18,20,22] to apply. These results indicate that more tightly packed compact structures are formed at moderate salt concentrations, while more open structures are formed at higher salt concentrations.

It is well-known[1] that polymers bound to colloid particles can impart stability through a steric mechanism (preventing the close approach of the colloid particles) or induce aggregation by "bridging" two or more particles. The amount of adsorbed polymer on the particle surface is a function of factors such as polymer molecular weight, hydrophobicity of the polymer, adsorption energy, solvent quality, and solution concentration. Bridging can occur only when the adsorbed amount of polymer is below saturation and the adsorbent surfaces are sufficiently close. The physical principle behind this phenomenon is that under the given conditions it is entropically more favorable to allow polymer chains to have contacts with the two proximate surfaces than subjecting their conformations to the restraint of contact with only one particle. At higher polymer concentrations all particles are fully covered, and the dangling tails and loops form a steric barrier against bridging flocculation. In view of these aspects, the salt-induced aggregation process of bare colloid particles is expected to be modulated by the presence of adsorbed polymer. The principal issue that will be addressed in this paper is how the structure of colloid aggregates and the kinetics of their formation in the presence of salt are influenced by adsorption of polymer.

For this purpose, we have used intensity (ILS) and dynamic (DLS) light scattering techniques to follow the salt-induced aggregation (most of the measurements have been carried out at a fixed salt concentration (0.7 M NaCl) where coagulation of the particles is observed) in aqueous suspensions of bare polystyrene latex particles and of particles covered with adsorbed layers of a hydrophobically modified ethyl(hydroxyethyl)-cellulose (HM-EHEC) or of its unmodified analogue (EHEC). Previous studies[26−31] have revealed that EHEC adsorbs extensively to hydrophobic surfaces. In a recent investigation,[32] results regarding structural and thermodynamic properties of semidilute aqueous solutions of EHEC and results concerning EHEC at the mica−water interface revealed the associative behavior of the EHEC chains. It was argued that the solutions contain both aggregates and individual EHEC coils.

The amount of adsorbed polymer onto the particle surface is expected to depend on the hydrophobicity of the polymer, and as a result of this, the aggregation process may be influenced. Unmodified EHEC polymer (without any nonylphenol groups) contains both hydrophilic and hydrophobic groups. From ILS experiments, the structural morphology (fractal dimension) can be probed, while from DLS the state and kinetics of aggregation can be characterized by determining the effective hydrodynamic particle diameters from the Stokes−Einstein equation.

Experimental Section

Colloidal Polystyrene Latex Particles. The monodisperse polystyrene latices were prepared by the F. K. Hansens group at the University of Oslo by emulsion polymerization under a stream of nitrogen at 80 °C using sodium dodecyl sulfate as emulsifier and potassium peroxosulfate as initiator. All the reagents employed were of analytical grade and were used without further purification. The method used in the preparation of the polystyrene latex particles has been described in detail elsewhere.[33] The latex contained 14% solids and was dialyzed for 2 weeks, with frequent changes of the dialysis water, in a cellulose dialysis tubing. The ζ potential was about -60 mV, and the negative ζ potential is due to sulfate groups on the particle surface. The stability of the colloidal suspensions before the addition of the salt was checked over 1 week by measurements of the mutual diffusion coefficient to ensure that irreversible aggregation of polystyrene spheres does not take place. In all experiments, the particle concentration of the latex suspension was maintained constant to the value of 0.001% w/w. The apparent hydrodynamic radius obtained from DLS through the Stokes−Einstein equation was 87 nm. The aggregation was induced by adding to the bare latex particle suspension or to the polymer/latex mixture an appropriate amount of uni-univalent electrolyte solution (0.7 M NaCl). One may suspect that the order of mixing may affect the results. However, no change in the values of the physical quantities was observed if salt was added to the polymer/latex mixtures or if the particles were added to the polymer/salt mixtures. The suspensions were homogenized by shaking the tubes.

Polymers. The EHEC and HM-EHEC samples were supplied from Akzo Nobel Surface Chemistry AB, Stenungsund, Sweden. Before use the polymers were purified as described elsewhere and stored in a desiccator.[34] Both the unmodified EHEC and the hydrophobically modified one (HM-EHEC) are ethyl-(hydroxyethyl)cellulose ethers with the same molecular weight (ca. $M_w \approx 100\,000$), and the degrees of substitution of ethyl and hydroxyethyl groups are $DS_{ethyl} = 0.8$ and $MS_{EO} = 1.8$, respectively. The values of DS and MS correspond to the average number of ethyl and hydroxyethyl groups per anhydroglucose unit of the polymer. The values of M_w, DS, and MS were all given by the manufacturer. The hydrophobically modified polymer is equivalent to the EHEC sample, but with branched nonylphenol chains grafted to the cellulose backbone. The degree of nonylphenol substitution was determined to be 1.7 mol % (ca. 6.5 groups per molecule) relative to the repeating units of the polymer by measuring the absorbance of the aromatic ring in nonylphenol at a wavelength of 275 nm with a Shimadzu UV-160 spectrophotometer. Phenol in aqueous solution was used as a calibration standard. A schematic illustration of the structure of EHEC and its hydrophobically modified analogue (HM-EHEC) is shown in Figure 1.

All samples were prepared by weighing the components, and the polymer was allowed to dissolve properly before mixed with the latex particles. Dust was removed from the samples by filtering the solutions directly into precleaned 10 mm NMR tubes (Wilmad Glass Co.) of highest quality.

Light-Scattering Measurements. The scattering process allows us to explore a system on a length scale of q^{-1}, where q is the wave vector defined as $q = 4\pi n \sin(\theta/2)/\lambda$. Here λ is the wavelength of the incident light in a vacuum, θ is the scattering angle, and n is the refractive index of the solution. The values of n were determined for all samples at $\lambda = 488$ nm by using an Abbé refractometer.

We used a standard, laboratory-built light-scattering spectrometer capable of both time-averaged scattered intensity and photon correlation measurements at different scattering angles. The beam from an argon ion laser (Spectra Physics model 2020),

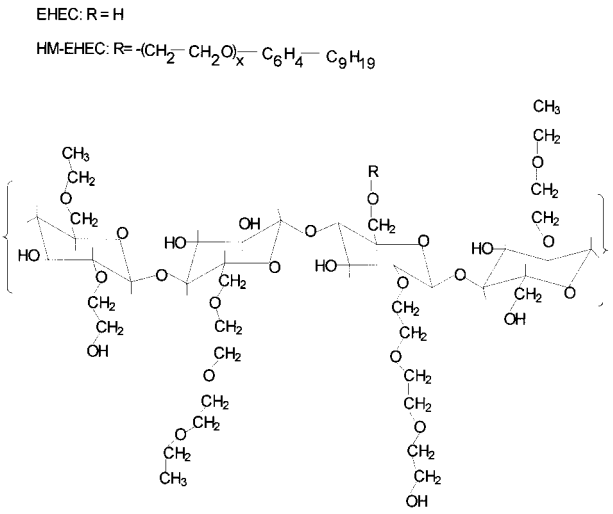

Figure 1. Schematic illustration of the structure of unmodified ethyl(hydroxyethyl)cellulose (EHEC) and its modified analogue (HM-EHEC).

operating at the wavelength $\lambda = 488$ nm with vertically polarized light, was focused on the sample cell through a temperature-controlled chamber filled with refractive index matching dibutyl phthalate. In all measurements the sample temperature was kept at 25.0 ± 0.05 °C. The light scattering experiments were carried out immediately after sample mixing in order to follow the structure morphology and the kinetic growth of the polystyrene latex clusters. Under the conditions of the present experiments, the scattered intensity from the colloid particles constituted a dominating feature, and the scattering intensity from the polymer could be neglected.

The intensity light scattering measurements were conducted using ALV (Langen-Germany) light scattering electronics in combination with the on-line program ODIL. The ILS experiments were performed at several scattering angles, and the total scattered intensity was recorded at each angle. The interval between each angle of measurement was 2°, the duration of each measurement was 8 s, and there were six repetitions at each angle. The most direct way to evaluate the clusters' fractal dimension d_f is via elastic light scattering, since the asymptotic behavior of the scattered intensity $I(q)$ is given by

$$I(q) \propto q^{-d_f} \quad (qR \gg 1) \tag{1}$$

Thus, the slope of the scattered intensity in the power-law regime gives the fractal dimension d_f.

In the DLS experiments, the full homodyne intensity autocorrelation function was determined with the aid of an ALV-5000 multiple-τ-digital correlator. The correlation functions were recorded in the real time "multiple-τ" mode of the correlator, in which 256 time channels are logarithmically spaced over an interval ranging from 0.2 μs to almost 1 h.

If the scattered field is assumed to exhibit Gaussian statistics, the experimentally recorded homodyne intensity autocorrelation function $g^2(q,t)$ is directly related to the theoretically amenable first-order electric field autocorrelation function $g^1(q,t)$ through the Siegert[35] relationship $g^2(q,t) = 1 + B|g^1(q,t)|^2$, where B (≤ 1) is an instrumental parameter.

For polydisperse systems, containing noninteracting particles with different size distribution, the nonexponential behavior of the autocorrelation function can be analyzed by methods such as the method of cumulants,[36] CONTIN,[37] or a Kohlrausch−Williams−Watts[38−40] stretched exponential function. The latter method has been reported[41−43] to be powerful in the analysis of correlation functions obtained from colloid systems, and the stretched exponential approach was also found to be successful in the description of the present correlation function data. The results presented in this work have been evaluated with the aid of the stretched exponential function, but a comparison with the other methods (method of cumulants and CONTIN) revealed that there is no significant difference between the values of the mutual diffusion coefficient determined from the different methods. The stretched exponential function employed in the analysis of the present correlation function data can be expressed in the following form

$$g^1(t) = \exp[-(t/\tau_{fe})^{\beta}] \tag{2}$$

where τ_{fe} is some effective relaxation time and β ($0 < \beta \leq 1$) is a measure of the width of the distribution of relaxation times. The width of the distribution decreases as β approaches 1. The values of β are about 0.95 in most cases and somewhat lower for particles in the presence of the highest polymer concentrations. In view of eq 2, the mean relaxation time is given by

$$\tau_f = (\tau_{fe}/\beta)\Gamma(1/\beta) \tag{3}$$

where $\Gamma(1/\beta)$ is the gamma function.

In the analysis of correlation function data, a nonlinear fitting algorithm (a modified Levenberg−Marquardt method) was used to obtain best-fit values of the parameters τ_{fe} and β appearing on the right-hand side of eq 2. From the mean relaxation time, we can calculate an apparent average hydrodynamic radius R_h of the clusters formed at finite concentrations by using the Stokes−Einstein relationship

$$R_h = \frac{k_B T}{6\pi\eta D} \tag{4}$$

where k_B is the Boltzmann constant, T is the absolute temperature, η is the viscosity of the medium, and the average mutual diffusion coefficient $D = 1/\tau_f q^2$. From the viscosity and the temperature, we could determine R_h of particles for various conditions. Each photon correlation measurement usually took about 2−3 min (at this time the correlation function has decayed), thus enabling us to follow closely the aggregate growth as a function of time. In most cases, our DLS measurements were carried out at a scattering angle of 30°. We should note that eq 4 is strictly valid only in the absence of interparticle interactions and internal motions, that is, $qR_h < 1$. For very large clusters, especially of nonspherical shape, some corrections to R_h should be made. Since we are more concerned with the characteristic kinetic growth of clusters rather than the real cluster size itself, this correction is not crucial. However, at different experimental conditions, we have carried out two independent kinetic growth measurements for the same system at two different scattering angles, i.e., 30° and 60°. The average hydrodynamic sizes measured as a function of time at the two scattering angles show some, but no significant, difference. When working with colloidal particles, multiple scattering may be a problem. At the present experimental conditions, we have not observed any signs of this effect.

Results and Discussion

We will first present and discuss the results from the salt-induced aggregation of the bare polystyrene latices. The effect of salt concentration on the time-dependent growth behavior of polystyrene aggregates is depicted in Figure 2a. A log−log plot of R_h vs time reveals that at low salt concentrations the

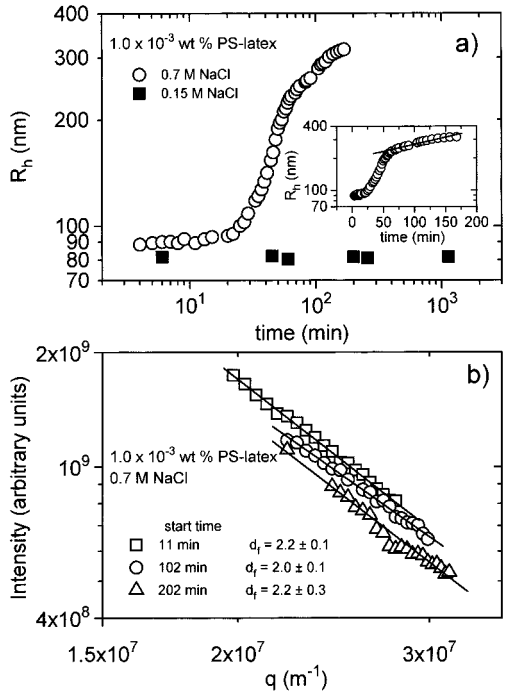

Figure 2. (a) Time evolution of R_h of the salt-induced aggregation of bare polystyrene latex particles at the conditions indicated. The linear behavior (the inset plot) at long times of polystyrene clusters in 0.7 M NaCl on the semilogarithmic plot indicates exponential kinetics of aggregation. (b) Plots of scattered intensity as a function of scattering vector for the times and conditions indicated. The linear behavior in the logarithmic plots is indicative of fractal aggregates.

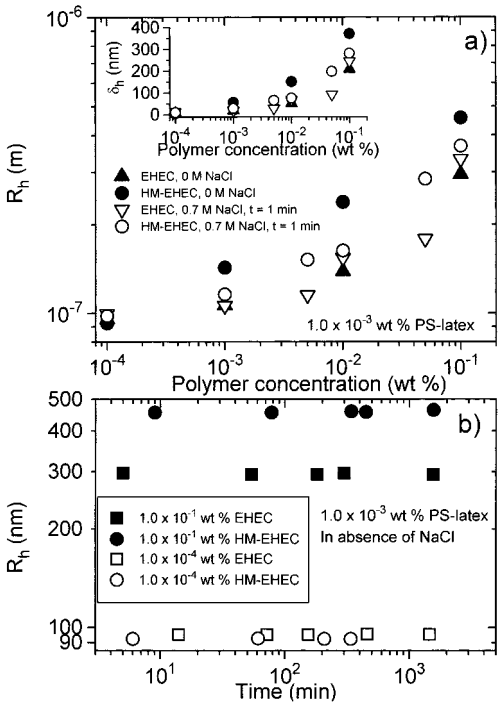

Figure 3. (a) Apparent hydrodynamic radius of polystyrene latex particles as a function of polymer concentration for the systems indicated. The inset plot shows the hydrodynamic thickness of the adsorbed layer as a function of polymer concentration for the same systems. (b) Time evolution of the apparent hydrodynamic radius of polystyrene latex particles in salt-free EHEC and HM-EHEC solutions at the concentrations indicated.

tendency of aggregation is absent (the repulsive forces between the particles are not yet screened), whereas at high salinity three different regimes of cluster growth can be discerned. During the very early times (the first 20 min) in aggregation (the initial stage) where the dominating clusters were of small size, the cluster growth process is slow. Actually, the cluster growth in the initial regime can be described by a power law $R_h \propto t^{\alpha}$ with $\alpha \approx 0.04$, showing linear behavior on the logarithmic graph. As will be discussed below, this is also a characteristic feature for polystyrene particles with adsorbed polymer at high salinity.

At longer times, a steep transition zone with a rapid growth of the clusters is observed, followed by a slower aggregation process at later times. The aggregation kinetics at long times seem to be exponential, as demonstrated by the linear behavior on the semilogarithmic plot shown in the inset of Figure 2a. A profile that is reminiscent of this has previously been reported[18,20] for salt-induced aggregation of polystyrene latex particles. The regime at long times is usually addressed in the study of the structural morphology and kinetics of colloids undergoing aggregation. The large deviations from the exponential kinetics noticed at early times in aggregation have been attributed[20] to the fact that the dominating clusters are of small size. Since the cluster size growth can be described by an exponential at later times, and the fractal dimension, determined from intensity light scattering, is close to 2.1 (see Figure 2b), the results indicate RLCA behavior. This finding is consistent with the results observed from previous studies[18,20,22] of salt-induced aggregation of bare polystyrene spheres at salt concentrations of the same magnitude as in the present case.

To find out whether the fractal structures of the clusters change as the aggregation proceeds, Figure 2b shows the linear behavior of scattered intensity against q in the logarithmic plots for the salt and particle concentration indicated at different times of commencement of the experiments. Since an ILS experiment takes about 20 min over the considered range of scattering angles, an incipient growth of the particles occurs. Within experimental error, the slopes are equal, yielding a d_f value of 2.1, which is consistent with the RLCA model. This result suggests that the fractal dimension is stable in time, indicating that the sticking probability is not largely changed as the clusters grow larger. In this context we should mention that ILS measurements have also been carried out on samples with the same concentration (0.001 wt %) of polystyrene latex particles but in the absence of salt, and in this case we observe, as expected, a fractal dimension close to 3. The finding that the sample with salt, even at early times, reveals an apparent fractal dimension of 2.1 may indicate the existence of large clusters.

By adding polymer to the latex system, the aggregation process is expected to be altered. The polymer concentration does not exceed 0.1 wt % because at higher concentrations the profile of the DLS correlation function becomes complex (two relaxation modes), and the colloid systems containing HM-EHEC and salt show signs of incipient phase separation. The overlap concentration of similar EHEC samples was estimated to be $c^* \approx 0.2$ wt %,[44,45] by using the relation $c^* = 1/[\eta]$, where $[\eta]$ is the intrinsic viscosity. This means that our experiments are performed in the dilute polymer concentration regime. The results in Figure 3a show that R_h of the particles increases gradually as the polymer concentration increases. This trend is a common feature at all conditions, for both EHEC and HM-EHEC in the presence and absence of salt, but is more pronounced for HM-EHEC.

Let us first consider the results in the absence of salt. It has previously been reported[26,27,29] that hydrophobic attraction between a EHEC polymer and the surface is the main driving force for adsorption. Thus, it can be anticipated that EHEC adsorbs extensively to substrate particles with hydrophobic surfaces, while adsorption is much lower[26,27] at a hydrophilic

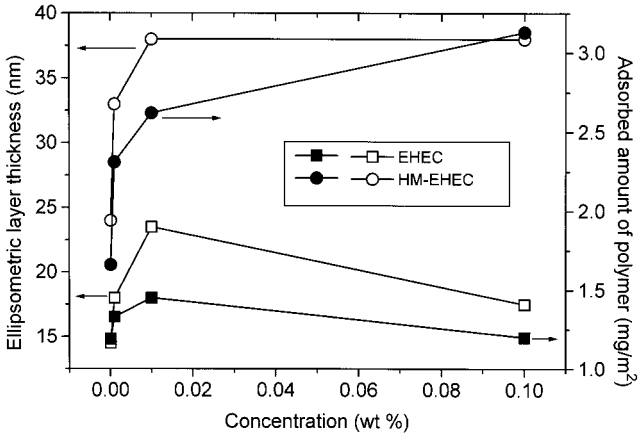

Figure 4. Adsorption isotherm and average ellipsometric layer thickness of EHEC and HM-EHEC on hydrophobized silica particles.

surface. It is expected that the most hydrophobic moieties, the ethyl groups, will be preferentially adsorbed onto the hydrophobic surfaces of the polystyrene latex spheres, whereas the hydrophilic regions of the polymer will orient toward the bulk, causing not only the segment density but also the distribution of the substituents to vary with the distance from the surface. This effect is probably strengthened by the fact that EHEC is not evenly substituted, but this polymer has a block character.

If we temporarily assume that no particle aggregation occurs during the polymer adsorption evolution, the hydrodynamic thickness of the adsorbed polymer layer, δ_h, can be calculated by subtracting the bare particle radius from that of the polymer-covered particle. This implies that δ_h increases strongly with polymer concentration (see Figure 3a and the inset plot). In fact, at the highest concentrations the calculated δ_h suggests that the adsorbed polymer layer may have a thickness of as much as 350 nm. We note that with the specified molecular weight and substitution degree the contour length of an individual polymer molecule is approximately 200 nm. One way to account for the observation is to introduce the concept of multiple-layer adsorption.[46−50] However, a recent ellipsometry study[31] of adsorption of EHEC and HM-EHEC onto hydrophobized silica surfaces does not support this interpretation. The results from this investigation are depicted in Figure 4, where the adsorbed amount of polymer and the average ellipsometric layer thickness δ_e are plotted as a function of polymer concentration. Initially, the adsorption rises steeply with polymer concentration and reaches a plateaulike region at ca. 1.5−1.75 and 2.5−3 mg/m^2 for EHEC and HM-EHEC, respectively. The plateaulike region is reached already at a low polymer concentration (ca. 0.01 wt %) for both polymers. The adsorption isotherms are hence of the high-affinity type, which frequently is observed for polymers. The fact that the amount of adsorbed polymer is much higher for HM-EHEC emphasizes the importance of the hydrophobic moieties for the adsorption process. Clearly, the values of the ellipsometric layer thicknesses are much lower than the corresponding values of the hydrodynamic layer thickness depicted in the inset plot of Figure 3a.

It is established[51] that the dominant contribution to the hydrodynamic layer thickness of adsorbed polymer comes from long tails, which extend far into the solution. Therefore, there is usually a discrepancy between layer thicknesses obtained from ellipsometry and DLS, which has been confirmed both experimentally[30,52,53] and theoretically.[51,54,55] However, the 10-fold difference, which we observe, is too large to be explained by differences between the two techniques alone. From the time evolution of the hydrodynamic radius, Figure 3b, it follows that a constant R_h is established within less than 10 min after mixing, while in the ellipsometry investigation a constant value of the layer thickness was reached after about 20 min. It should also be noted that experimental details such as hydrodynamic conditions (stirring) suggest that ellipsometry should yield a faster adsorption evolution than DLS.

If we assume that all polymer material is adsorbed onto the particles, we can, on the basis of the ellipsometry data, estimate the limit when the particles are coated with polymer. The calculation suggests that the particles will be completely covered at polymer concentrations above 10^{-4} wt %. Here, bridging is expected to be suppressed. However, also in solutions where the polymer concentration is well above this limit, particle aggregation caused by "nonequilibrium" effects, such as bridging flocculation, cannot be ruled out. Even though long-term stability (metastability) may be expected in these systems, the slow kinetics of the adsorption process may give rise to a different scenario. As long as the polymers not fully cover the particle surfaces (equilibrium adsorption is not reached), the probability of bridging to another particle can be significant. This implies that the adsorbed polymer layer should be extended and the bridging force strong enough to overcome the long-range electrostatic repulsion between the particles in salt-free solutions. Also, the collisions between the particles has to be frequent enough to produce a significant number of aggregates during the time interval where bridging dominates the interaction. The bridging mechanism is therefore important at times shorter than the adsorption equilibrium time. At longer times, no bare surface sites are exposed, and the aggregation process due to bridging stops. This model accounts for the observed time evolution of the hydrodynamic radius of the particles (Figure 3b) and also explains the large discrepancy between the hydrodynamic and ellipsometric layer thicknesses (Figures 3 and 4).

It is evident from Figure 3a that the hydrodynamic radius of the particles at the lowest polymer concentration is close to the value for bare particles. These features indicate that the polymers lie rather compact on the surfaces of the particles at low polymer concentration. The lowest polymer concentration is close to the saturation limit, which suggests that bridging is possible, but on the other hand, the layers may not extend beyond the range of the electrostatic repulsion. At higher polymer concentrations the adsorbed polymer chains reach further out from the surface, as suggested by the ellipsometric data (Figure 4).

The adsorption characteristics of EHEC and HM-EHEC on polystyrene latex particles are expected to be affected by cosolutes, like alcohols, surfactants, and salts. Depending on the additive, the thermodynamic conditions of the system and electrostatic interactions may be modified. Figure 3a shows the effect of salt addition (the NaCl concentration is the same (0.7 M) as that utilized in the aggregation of the bare polystyrene latices) on the hydrodynamic radius of the particles with adsorbed EHEC and HM-EHEC. The results indicate that there is practically no, or a small, effect of the salt addition on the thickness of the adsorbed EHEC layer, while a significant decrease of the thickness of the adsorbed HM-EHEC layer is observed at higher polymer concentrations in the presence of salt. These findings can probably be rationalized in terms of changed thermodynamic conditions upon addition of salt. It has previously been found[56,57] that, on addition of NaCl to an EHEC/water solution or a HM-EHEC/water solution, the cloud point is decreased, and as a result the polymer molecules cluster together and there is a decrease in the solubility of the polymer molecules. Phase separation at room temperature is observed

at a lower NaCl concentration for the hydrophobically modified analogue. Furthermore, the hydrophobicity of the polymer is expected to be promoted by NaCl addition, and the level of adsorption of the polymer onto the polystyrene latex spheres rises.[26]

In light of these aspects, the conjecture for the present EHEC−water−polystyrene latex system is that the enhanced adsorption induced through the addition of NaCl (0.7 M) is masked by the contraction[30] of the adsorbed layer thickness of EHEC as a result of poorer thermodynamic conditions (weak excluded-volume effects) when salt is added. As a consequence of this compensation effect, the thickness of the adsorbed EHEC layer is virtually intact upon salt addition. In the case of HM-EHEC in the presence of salt, the thermodynamic conditions are further deteriorated (approaching phase separation) as the polymer concentration increases, and the strong compression of the hydrodynamic layer dominates over the increased adsorption of HM-EHEC. This leads to the observed reduction of the hydrodynamic thickness for HM-EHEC at higher polymer concentration in the presence of salt. The surmise that the thermodynamic conditions are poorer for the systems with the hydrophobically modified polymer than those with the unmodified analogue is supported by the fact that when the salinity (0.7 M) and the latex particle concentration (0.001 wt %) are kept constant, an incipient phase separation (signs of turbidity) is observed in the dispersion as the HM-EHEC concentration is increased above 0.1 wt %. No signs of phase separation could be detected under the corresponding conditions in dispersions containing EHEC.

The characteristic features of the salt-induced aggregation of bare polystyrene latex spheres can be expected to be affected by the adsorption of polymer onto the particles. One can envisage that factors such as the thickness of the adsorbed layer, the conformation of the adsorbed chains, and the hydrophobicity of the adsorbed polymer will influence the salt-induced aggregation behavior of the polystyrene latex particles. This issue is addressed in Figure 5, where the time evolution of the apparent hydrodynamic radius during the salt-induced (0.7 M) processes occurring in EHEC-coated and HM-EHEC-coated polystyrene latex (0.001 wt %) suspensions is depicted for different EHEC and HM-EHEC concentrations. The cluster size growth can, over an extended time domain, be described by a power law (a linear dependence in a double-logarithmic plot) $R_h \propto t^{\alpha}$, with the exponent $\alpha \approx 0.04$ for both EHEC and HM-EHEC over a broad polymer concentration range (1.0×10^{-4}−0.1 wt %). We may note that this value of the power law exponent is the same as that observed during the initial stage of the salt-induced aggregation process of the bare polystyrene latex particles. It should be mentioned that even if the time evolution of R_h for the polymer-coated particles was followed over a week, no change in the power law behavior to faster growth kinetics was detected. This shows that the slow aggregation regime, described by a power law, exists for a remarkable length of time. The resemblance between the cluster size growth of the bare polystyrene latex spheres in the early stage of the aggregation process and the long-time evolution of R_h of the polymer-coated particles may be fortuitous, but it cannot be excluded that these processes may have the same physical origin. It is possible that when polymer is adsorbed to the particles, the formation of large clusters is suppressed due to steric hindrance and geometrical reasons. As a result, the formation of small clusters is favored during the time evolution of the aggregation process.

It is well-known[1,58] that added polymers that bind to the

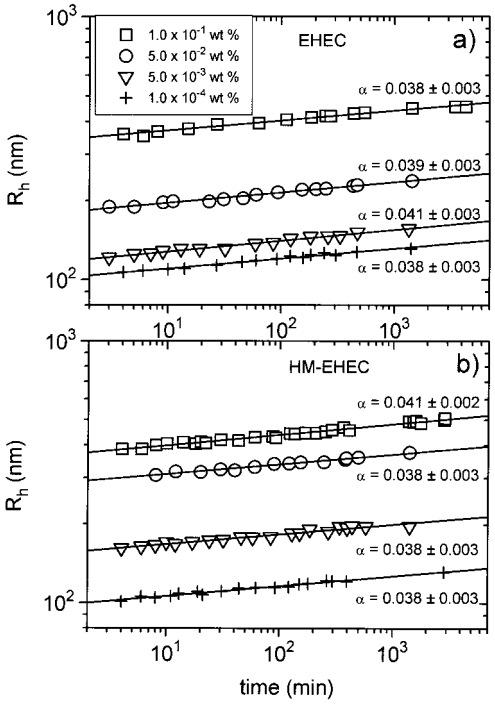

Figure 5. Time evolution (log−log plot) of the apparent hydrodynamic radius of polymer-covered polystyrene latex particles in the presence of NaCl (0.7 M) at the polymer concentrations indicated: (a) EHEC, (b) HM-EHEC. The slopes yield the power law exponent α.

colloidal particles may prevent strong aggregation by offering a steric barrier to close approach. The present findings suggest that salt-induced aggregation of the polystyrene latex particles can be strongly slowed by small amounts of polymer. Although, to the best of our knowledge, no scaling law has been reported for the cluster size growth of polymer-covered latex particles in the presence of salt, it has been noted[5,6,59−63] that the salt-induced aggregation rate of colloid particles may be slowed if polymer is adsorbed. In a recent light scattering investigation[64] on salt-induced aggregation of colloidal particles, it was shown that the aggregation process of the latex particles can be prevented or reversed in the presence of small amounts of the nonadsorbing sodium poly(stryrenesulfonate) polymer. In this study we have not carried out measurements at polymer concentrations below 10^{-4} wt %, because it is difficult to obtain reproducible results, probably due to adsorption of polymer onto, e.g., the glass walls of the measuring tubes at these very low concentrations.

The results presented in Figure 5 indicate a unitary behavior of the apparent hydrodynamic radius, with a power law exponent that is independent of hydrophobicity of the cellulose derivative and of polymer concentration in the dilute regime. To illustrate this aspect, the reduced apparent hydrodynamic radius $(R_h - R_{h,1\ min})/R_{h,1\ min}$ is plotted as a function of time in Figure 6. R_h is the hydrodynamic radius of the cluster at time t and $R_{h,1\ min}$ is the hydrodynamic radius 1 min after the start of the aggregation process. We can see that the early stage of the aggregation process of the bare particles and the cluster size growth of the polymer-coated particles over an extended time yield a master curve. The condensation of the data onto a master curve suggests a universal feature, independent of adsorbed layer thickness and hydrophobicity of the polymer, of the slow aggregation process. This remarkable finding shows that only a small amount of adsorbing polymer is needed to profoundly affect the kinetics of the salt-induced aggregation process of the latex particles.

Figure 7 depicts the q dependence of the scattered intensity

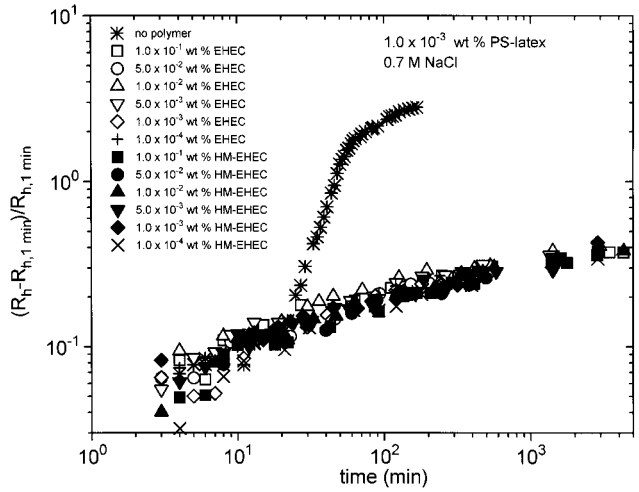

Figure 6. Reduced hydrodynamic radius as a function of time for the salt-induced aggregation of the systems indicated. A universal behavior can be observed.

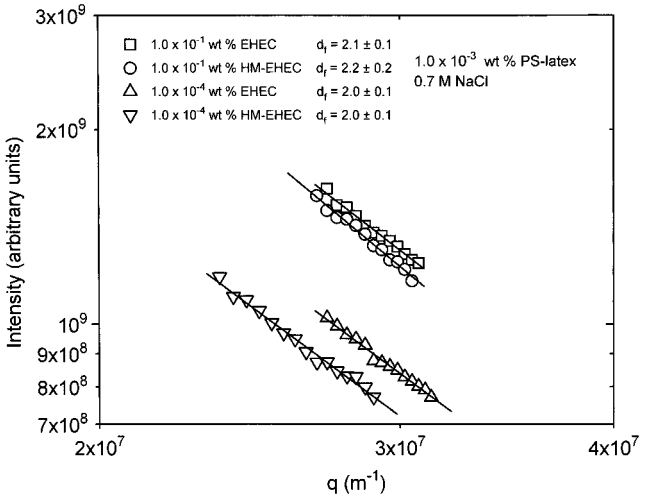

Figure 7. Plots of scattered intensity as a function of scattering vector for a low and a high concentration of EHEC and HM-EHEC in the presence of 0.7 M NaCl. The linear behavior in the logarithmic plots is indicative of fractal aggregates, and the slopes yield a fractal dimension of about 2.1.

for salt-induced aggregation of latex particles in the presence of EHEC and HM-EHEC of two different concentrations. These results yield at all conditions a fractal dimension close to 2.1. This value is the same as that found for the bare polystyrene particles at different stages during the salt-induced aggregation process. These results imply that the nature and thickness of the adlayers do not influence the fractal morphology of the cluster structures. Although the kinetics of the salt-induced aggregation process of polystyrene latex particles is significantly altered when a polymer that adsorbs onto the spheres is added to the dispersion, the fractal dimension of 2.1 is intact, suggesting that the sticking probability of clusters approaches zero. There are some previous studies where the fractal dimension of EHEC systems has been addressed. In an intensity light scattering study[65] on semidilute aqueous solutions of EHEC and HM-EHEC in the presence of an anionic surfactant, a fractal dimension of 1.6 was reported. In a recent transmission electron microscopy study,[66] EHEC was used as a stabilizer for the dispersion polymerization of aniline in water−ethanol mixtures. When the dispersions were exposed to ultrasound, unstable nanoparticles were generated. These particles undergo fractal aggregation with fractal dimensions in the range 1.7−1.9, depending on the environmental conditions.

Summary and Conclusions

Intensity light scattering offers an effective tool for the determination of the fractal dimension of aggregates of colloidal particles. Dynamic light scattering can be used to probe the hydrodynamic radius of the aggregates and to monitor the aggregation kinetics. The two approaches are supplementary to each other. The ILS experiments carried out on salt-induced aggregation of bare polystyrene latex particles and particles covered with various amounts of EHEC or HM-EHEC revealed at all conditions a fractal dimension of 2.1.

The salt-induced kinetic cluster growth of bare latex particles was characterized by the apparent hydrodynamic radius, and three regimes could be discerned. At early times a slow aggregation process is detected, which can be described by a power law $R_h \propto t^{0.04}$, and at longer times a steep transition occurred to a long-time behavior characterized by exponential kinetics of aggregation. In the presence of EHEC or HM-EHEC the salt-induced aggregation kinetics of the dispersions is altered in a remarkable way. In this case, the cluster size growth is very slow over the entire time domain (up to 1 week) and can be described by a power law $R_h \propto t^{0.04}$. The value of the power law exponent is independent of the hydrophobicity of the polymer and of polymer concentration in the dilute regime (10^{-4}−0.1 wt %). A feature of universality emerges from these results. It can be concluded that only a small amount of polymer (10^{-4} wt %) is needed to slow the salt-induced aggregation kinetics of the polystyrene latex spheres.

In the absence of salt, the apparent hydrodynamic radius of the particles increases with increasing polymer concentration, and this tendency is more pronounced for the hydrophobically modified polymer. Upon addition of salt, the hydrodynamic layer thickness of EHEC is almost unaffected, while the adsorbed layer of HM-EHEC contracts considerably at higher polymer concentrations. The conjecture is that the enhanced amount of polymer adsorbed to the particles as a result of salt addition is for EHEC compensated by the decrease of the adsorbed layer thickness due to worsening thermodynamic conditions, while for HM-EHEC the thermodynamic conditions approach phase separation, and in this case the contraction of the adsorbed layer dominates.

References and Notes

(1) Napper, D. H. *Polymeric Stabilization of Colloidal Dispersions*; Academic Press: London, 1983.

(2) Cohen Stuart, M A.; Cosgrove, T.; Vincent, B. *Adv. Colloid Interface Sci.* **1986**, *24*, 143.

(3) Milner, S. T. *Science* **1991**, *251*, 905.

(4) Halperin, A.; Tirrell, M.; Lodge, T. P. *Adv. Polym. Sci.* **1992**, *100*, 31.

(5) Einarson, M. B.; Berg, J. C. *J. Colloid Interface Sci.* **1993**, *155*, 165.

(6) Killmann, E.; Bauer, D.; Fuchs, A.; Portenlänger, O.; Rehmet, R.; Rustemeier, O. *Prog. Colloid Polym. Sci.* **1998**, *111*, 135.

(7) Witten, Jr., T. A.; Sander, L. M. *Phys. Rev. Lett.* **1981**, *47*, 1400.

(8) Meakin, P. *Phys. Rev. Lett.* **1983**, *51*, 1119.

(9) Brown, W. D.; Ball, R. C. *J. Phys. A* **1985**, *18*, L 517.

(10) Martin, J. E.; Ackerson, B. J. *Phys. Rev. A* **1985**, *31*, 1180.

(11) Jullien, R.; Botet, R.; Mors, P. M. *Faraday Discuss. Chem. Soc.* **1987**, *83*, 125.

(12) Schaefer, D. W.; Martin, J. E.; Wiltzius, P.; Cannell, D. S. *Phys. Rev. Lett.* **1984**, *52*, 2371.

(13) Masushita, M.; Sumida, K.; Sawada, Y. *J. Phys. Soc. Jpn.* **1985**, *54*, 2786.

(14) Aubert, C.; Cannell, D. S. *Phys. Rev. Lett.* **1986**, *56*, 738.

(15) Bolle, G.; Cametti, C.; Codastefano, P.; Tartaglia, P. *Phys. Rev. A* **1987**, *35*, 837.
(16) Tang, P.; Colflesh, D. E.; Chu, B. *J. Colloid Interface Sci.* **1988**, *126*, 304.
(17) Majolino, D.; Mallamace, F.; Migliardo, P.; Micali, N.; Vasi, C. *Phys. Rev. A* **1989**, *40*, 4665.
(18) Lin, M. Y.; Lindsay, H. M.; Weitz, D. A.; Ball, R. C.; Klein, R.; Meakin, P. *Nature* **1989**, *339*, 360.
(19) Martin, J. E.; Wilcoxon, J. P.; Schaefer, D.; Odinek, J. *Phys. Rev. A* **1990**, *41*, 4379.
(20) Zhou, Z.; Chu, B. *J. Colloid Interface Sci.* **1991**, *143*, 356.
(21) Asnaghi, D.; Carpineti, M.; Giglio, M.; Sozzi, M. *Phys. Rev. A* **1992**, *45*, 1018; *Prog. Colloid Polym. Sci*. **1992**, *89*, 60.
(22) Burns, J. L.; Yan, Y.; Jameson, G. J.; Biggs, S. *Langmuir* **1997**, *13*, 6413.
(23) Kolb, M.; Botet, R.; Jullien, R. *Phys. Rev. Lett.* **1983**, *51*, 1123.
(24) Julien, R.; Kolb, M. *J. Phys. A* **1984**, *17*, L776.
(25) Weitz, D. A.; Huang, J. S.; Lin, M. Y.; Sung, J. *Phys. Rev. Lett.* **1985**, *54*, 1416.
(26) Malmsten, M.; Lindman, B. *Langmuir* **1990**, *6*, 357.
(27) Malmsten, M.; Claesson, P. M.; Pezron, E.; Pezron, I. *Langmuir* **1990**, *6*, 1572.
(28) Malmsten, M.; Claesson, P. M. *Langmuir* **1991**, *7*, 988.
(29) Malmsten, M.; Lindman, B.; Holmberg, K.; Brink, C. *Langmuir* **1991**, *7*, 2412.
(30) Tiberg, F.; Malmsten, M. In *Cellulose and Cellulose Derivatives: Physico-Chemical Aspects and Industrial Applications*; Kennedy, J. F., Phillips, G. O., Williams, P. A., Eds.; Woodhead Publishing Ltd.: Cambridge, U.K., 1995; pp 363−369.
(31) Joabsson, F.; Thuresson, K.; Lindman, B. Unpublished results.
(32) Freyssingeas, E.; Thuresson, K.; Nylander, T.; Joabsson, F.; Lindman, B. *Langmuir* **1998**, *14*, 5877.
(33) Hansen, F. K.; Evenrød, A. *Fremstilling av seed for MPP*; DYNO Industries: Lillestrøm, Norway, 1983.
(34) Thuresson, K.; Karlström, G.; Lindman, B. *J. Phys. Chem.* **1995**, *99*, 3823.
(35) Siegert, A. J. F. Massachusetts Institute of Technology, Rad. Lab. Rep. No. 465, 1943.
(36) Koppel, D. E. *J. Chem. Phys.* **1972**, *57*, 4814.
(37) Provencer, S. W. *Biophys. J.* **1976**, *16*, 27; *J. Chem. Phys.* **1976**, *64*, 2772; *Makromol. Chem.* **1979**, *180* 201.
(38) Kohlrausch, R. *Prg. Ann. Phys.* **1847**, *12*, 393.
(39) Williams, G.; Watts, D. C. *Trans. Faraday Soc.* **1970**, *66*, 80.
(40) Ngai, K. L. *Adv. Colloid Interface Sci.* **1996**, *64*, 1.
(41) Phillies, G. D. J.; Richardson, C.; Quinlan, C. A.; Ren, S. Z. *Macromolecules* **1993**, *26*, 6849.
(42) Ngai, K. L.; Phillies, G. D. J. *J. Chem. Phys.* **1996**, *105*, 8385.
(43) Phillies, G. D. J.; Lacroix, M. *J. Phys. Chem. B* **1997**, *101*, 39.
(44) Holmberg, C.; Nilsson, S.; Singh, S. K.; Sundelöf, L.-O. *J Phys. Chem.* **1992**, *96*, 871.
(45) Kabalnov, A.; Olsson, U.; Thuresson, K.; Wennerström, H. *Langmuir* **1994**, *10*, 4509.
(46) Tanaka, R.; Meadows, J.; Phillips, G. O.; Williams, P. A. In *Cellulose-Structural and Functional Aspects*; Kennedy, J. F., Phillips, G. O., Williams, P. A., Eds.; Ellis Horwood: Chichester, U.K., 1989; pp 329−335.
(47) Tanaka, R.; Williams, P. A.; Meadows, J.; Phillips, G. O. *Colloids Surf.* **1992**, *66*, 63.
(48) Jenkins, R. D.; Durali, M.; Silebi, C. A.; El-Aaser, M. S. *J. Colloid Interface Sci.* **1992**, *154*, 502.
(49) Argillier, J.-F.; Audibert, A.; Lecourtier, J.; Moan, M.; Rousseau, L. *Colloids Surf. A: Physicochem. Eng. Aspects* **1996**, *113*, 247.
(50) Volpert, E.; Selb, J.; Candau, F.; Green, N.; Argillier, J. F.; Audibert, A. *Langmuir* **1998**, *14*, 1870.
(51) Cohen Stuart, M. A.; Waajen, F. H. W. H.; Cosgrove, T.; Vincent, B.; Crowley, T. L. *Macromolecules* **1984**, *17*, 1825.
(52) Takahshi, A.; Kawaguchi, M.; Kayashi, K.; Kato, T. *ACS Symp. Ser.* **1984**, *No. 240*, 39.
(53) Barnett, K. G.; Cosgrove, T.; Vincent, B.; Burgess, A. N.; Crowley, T. L.; King, T.; Turner, J. D.; Tadros, Th. F. *Polymer* **1981**, *22*, 283.
(54) Varoqui, R.; Dejardin, P. *J. Chem. Phys.* **1977**, *66*, 4395.
(55) Takahashi, A.; Kawaguchi, M. *Adv. Polym. Sci.* **1982**, *46*, 1.
(56) Thuresson, K.; Nilsson, S.; Lindman, B. In *Cellulose and Cellulose Derivatives: Physico-Chemical Aspects and Industrial Applications*; Kennedy, J. F., Phillips, G. O., Williams, P. A., Eds.; Woodhead Publishing: Ltd.: Cambridge, U.K., 1995; pp 323−329.
(57) Thuresson, K.; Nilsson, S.; Lindman, B. *Langmuir* **1996**, *12*, 2412.
(58) Dickinson, E.; Eriksson, L. *Adv. Colloid Interface Sci.* **1991**, *34*, 1.
(59) Killmann, E.; Maier, H.; Baker, J. A. *Colloids Surf.* **1988**, *31*, 51.
(60) Seebergh, J. E.; Berg, J. C. *Langmuir* **1994**, *10*, 454.
(61) Rustemeier, O.; Killmann, E. *J. Colloid Interface Sci.* **1997**, *190*, 360.
(62) Wind, B.; Killmann, E. *Colloid Polym. Sci.* **1998**, *276*, 903.
(63) Di Biasio, A.; Bordi, F.; Cametti, C.; Codastefano, P. *J. Chem. Soc., Faraday Trans.* **1998**, *94*, 3477.
(64) Jamil, T.; Russo, P. S. *Langmuir* **1998**, *14*, 264.
(65) Thuresson, K.; Nyström, B.; Wang, G.; Lindman, B. *Langmuir* **1995**, *11*, 3730.
(66) Chattopadhyay, D.; Banerjee, S.; Chakravorty, D.; Mandal, B. M. *Langmuir* **1998**, *14*, 1544.